sciendo

The EuroBiotech Journal

RESEARCH ARTICLE

Omics Sciences

Improved micro-impedance spectroscopy to determine cell barrier properties

Md. Mehadi Hasan Sohag[1], Olivier Nicoud[1,2], Racha Amine[1], Abir Khalil-Mgharbel[2], Jean-Pierre Alcaraz[1], Isabelle Vilgrain[2*] and Donald K Martin[1*]

Abstract

The goal of this study was to determine whether the Tethapod system, which was designed to determine the impedance properties of lipid bilayers, could be used for cell culture in order to utilise micro-impedance spectroscopy to examine further biological applications. To that purpose we have used normal epithelial cells from kidney (RPTEC) and a kidney cancer cell model (786-O). We demonstrate that the Tethapod system is compatible with the culture of 10,000 cells seeded to grow on a small area gold measurement electrode for several days without affecting the cell viability. Furthermore, the range of frequencies for EIS measurements were tuned to examine easily the characteristics of the cell monolayer. We demonstrate significant differences in the paracellular resistance pathway between normal and cancer kidney epithelial cells. Thus, we conclude that this device has advantages for the study of cultured cells that include (i) the configuration of measurement and reference electrodes across a microfluidic channel, and (ii) the small surface area of 6 parallel measurement electrodes (2.1 mm^2) integrated in a microfluidic system. These characteristics might improve micro-impedance spectroscopy measurement techniques to provide a simple tool for further studies in the field of the patho-physiology of biological barriers.

Keywords: Electrical impedance spectroscopy; cell monolayer; renal proximal tubule epithelial cell; cancerous kidney cell

[1]University Grenoble Alpes, SyNaBi, TIMC-IMAG/CNRS/INSERM, UMR 5525, F-38000 Grenoble, France

[2]University Grenoble Alpes, IMAC, INSERM (UMR_S 1036), CEA, IRIG-BCI, F-38000, Grenoble, France

*Co-Corresponding authors:
I. Vilgrain (isabelle.vilgrain@cea.fr) and
D. K. Martin
(don.martin@univ-grenoble-alpes.fr)

DOI: 10.2478/ebtj-2020-0017

Introduction

Over the last decade, the development of micro-dimensional systems to improve microscale measurements has attracted enormous attention due to their portability, high accuracy, and short response time. Consequently, they have evolved to a miniaturized automated version of biological measurements usually termed "Lab-on-Chip". Impedance spectroscopy is a measurement technique that is very useful to characterize several electrical properties of materials and their interfaces with electrically conducting electrodes. It may be used to determine the dynamics of bound or mobile charges in the bulk or interfacial regions of any kind of solid or liquid material, including ionic, semiconducting, mixed electronic-ionic, and even insulators (dielectrics). Electrical measurements can evaluate the electrochemical behavior of electrode and/or electrolyte materials for living cells (1, 2). Indeed several devices have been developed over the last ten years that have minimized the number of cells for the analysis and also have reduced the response time to identify differences in cell behavior, such as monitoring of cell adhesion, spreading and motility of anchorage-dependent cells (3). Systems for impedance spectroscopy have also been designed for the analysis of single cells in suspension (4). Nonetheless, the barrier properties of epithelial cells are essential for their physiology and such measurements must be done on cell monolayers.

We have previously used the Tethapod system (SDX Tethered Membranes, Australia) to determine the impedance properties of lipid bilayers (5). The goal of this study was to determine whether this microdevice could be used for cell culture in order to measure

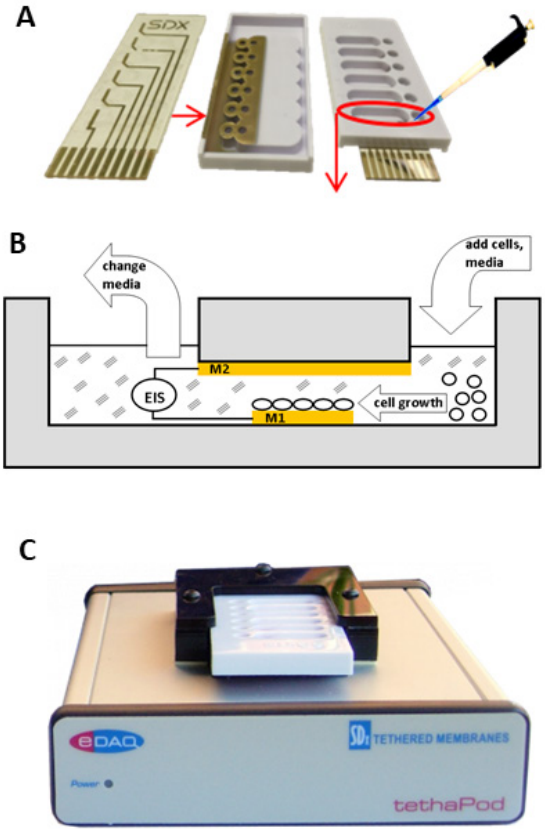

Figure 1. The electrical impedance spectroscopy (EIS) system. **(A)** The assembly of the microscope slide for the T10 electrode chip with its pattern of gold electrodes, and the microfluidic cartridge. Note that the slide for the T10 electrode is transparent and the gold tracks are sufficiently thin to be transparent. The red circle shows the entry and exit ports for the microfluidic channel that encloses the measurement electrode. **(B)** Cross-section of one microfluidic channel and ports. The arrow labelled as the entry of cells and media is via the small entry port of panel A. The cells migrate onto the gold measurement electrode (during 24 hours). The space between the electrodes is completely filled with media. The total capacity of the microfluidic chamber is 400µl. The media is changed by aspiration from the larger port of panel A. The gold measuring electrode is marked **M1** and the gold reference electrode is marked **M2. (C)** The assembled microfluidic cartridge is inserted into the Tethapod reader and the EIS measurements are achieved using the 2 electrodes M1 and M2.

impedance spectroscopy for further biological applications. To that purpose we have used normal epithelial cells from kidney (RPTEC) and a kidney cancer cell model (786-O).

Methods

Cell culture

Two types of epithelial cells from kidney were used in this study: the renal proximal tubule epithelial cells (RPTEC) and the tumour model of renal cell carcinoma (786-O cells). The normal RPTEC cells were purchased from (Evercyte GmbH) and grown at 37°C in ProXup medium. The 786-O tumour cells were purchased from Lonza and grown at 37°C in RPMI medium supplemented with fetal bovine serum (10%).

Electrical Impedance Spectroscopy (EIS) measurements

EIS measurements were performed using the Tethapod system (SDX Tethered Membranes, Australia). This system is usually used for EIS for measurements of the impedance properties of lipid bilayers (5). We used the T10 electrode chips that are supplied for use in the Tethapod. The T10 electrode chips had a pattern of gold electrodes that were supplied with a pre-coating of a stable monolayer that comprised a mixture of ester-free DLP ($C_{49}H_{92}O_{11}S_2$) and BnSS TEG ($C_{15}H_{24}O_4S_2$) molecules in the molar ratio of 10:90.

Results

Cell culture on the micro-impedance spectroscopy device

Renal proximal tubule epithelial cells (RPTEC) and renal cell carcinoma tumour cells (786-O) have been chosen in this study as they represent normal and tumour cells of the human kidney. Identifying distinct properties between normal and tumour cells is a major goal in cancer. These cells have been largely used in cell biology to study specific biological parameters such as cell proliferation, migration, and invasion as well as to determine specific potential targets to treat kidney cancer. The T10 electrode chip is provided in 100% ethanol. Prior to seeding of the cells the T10 electrode chips and the supplied microfluidic cartridge were incubated for 30 minutes in ethanol 70% to be adapted for cell culture. The T10 electrode chips and the microfluidic cartridge were dried thoroughly, and then

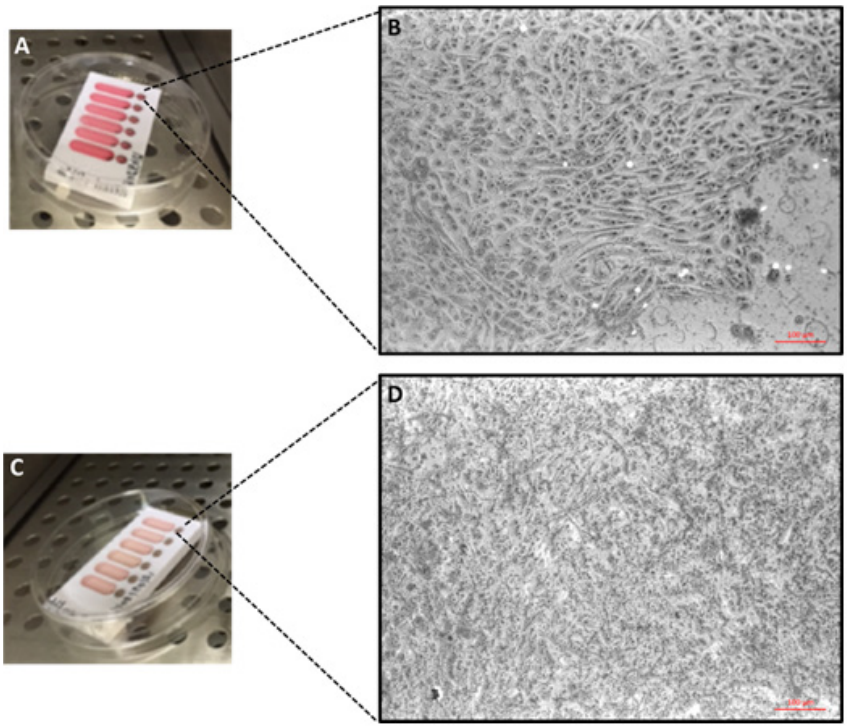

Figure 2. (A) EIS microfluidic cartridge seeded with the normal renal proximal tubule epithelial cells (RPTEC) in the Proxup medium adapted for their growth in culture. **(B)** Phase-contrast image of normal renal proximal tubule epithelial cells (RPTEC) after growing for 3 days on the electrodes of the EIS microfluidic cartridge. Note that these gold electrodes were thin enough to allow light to pass through for these images. **(C)** EIS microfluidic cartridge seeded with the renal cell carcinoma tumor cells (786-O) in RPMI medium supplemented with fetal bovine serum (10%). This is a different medium to that of the RPTEC cells, hence the difference in colour. **(D)** Phase-contrast image of renal cell carcinoma tumor cells (786-O) after growing for 3 days on the electrodes of the EIS microfluidic cartridge. Note that the growth of these tumour cells is less organized than the RPTEC normal cells.

the T10 electrode chip was assembled with the microfluidic cartridge (**Figure 1**).

The electrodes were then coated with fibronectin (7 µg/mL) for 30 minutes at 37°C using the entry ports of the microfluidic cartridge. After rinsing the fibronectin with culture media 10,000 cells of each type were seeded onto 5 wells of a T10/microfluidic cartridge in 200 µL of culture medium, and culture medium alone (no cells) was added to the 6th well. The T10/microfluidic cartridge was incubated at 37°C and 5% CO_2 for 3 days, with the durations indicated in text and figure legends.

As shown in **Figure 2 (A,C)**, the EIS microfluidic cartridges were enclosed in petri dishes before being placed in the incubator of the tissue culture room. Phase-contrast images were recorded after 3 days of culture for both the normal RPTEC and the tumor cells 786-O, as illustrated in **Figure 2 (B,D)**. These images demonstrate that the two cell types were able to grow onto the gold measurement electrode and to reach almost confluency within 2 to 3 days. No toxic effect of the electrode was detected, which demonstrates that this device is compatible with cell culture. The EIS measurements were then performed.

Micro-impedance spectroscopy

To perform the EIS measurements using the Tethapod, the T10/microfluidic cartridge was removed briefly from the incubator after 1, 2 and 3 days. On the second day, after the EIS measurement, fresh medium was added to each well after carefully aspirating the old medium. The experiments were repeated on 3 separate occasions with different T10/microfluidic cartridges. With 5 electrodes used in each T10/microfluidic cartridge, the experiments were performed over 15 separate cell monolayers for each type of cell.

The total impedance signal was modelled using the equivalent circuit shown in **Figure 3**. The paracellular resistance is represented by R_n and the capacitance of the cell monolayer is represented by C_n. The other components take into account the impedance contributions of the electrodes (CPE_m, R_m) and the media solution (R_e, C_c). The modelling was achieved using the TethaQuick software (v2.0.49) using amplitude weighting. The application of this model is illustrated for examples of EIS measurements made at day 1 for the RPTEC and 786-O cells (**Figure 3B, 3C**). In these example for the RPTEC cells the values for the equivalent circuit are R_e = 516Ω, Cs = 0.82µF, R_m = 250kΩ; the CPE_m values are Qm = 0.92µF.s$^{(\alpha-1)}$ and α_m = 0.83, R_n = 2382kΩ, and C_n = 0.76µF. In this example for the 786-O cells the values for the equivalent circuit are R_e = 366Ω, C_s = 1.58µF, R_m = 101kΩ; the CPE_m values are Qm = 1.38µF.s$^{(\alpha-1)}$ and α_m = 0.83, R_n = 542kΩ, and C_n = 2.18µF.

The results for the EIS measurement are presented in **Figure 4**. These data were tested for statistical significance using a 2-way ANOVA for resistance and for capacitance performed

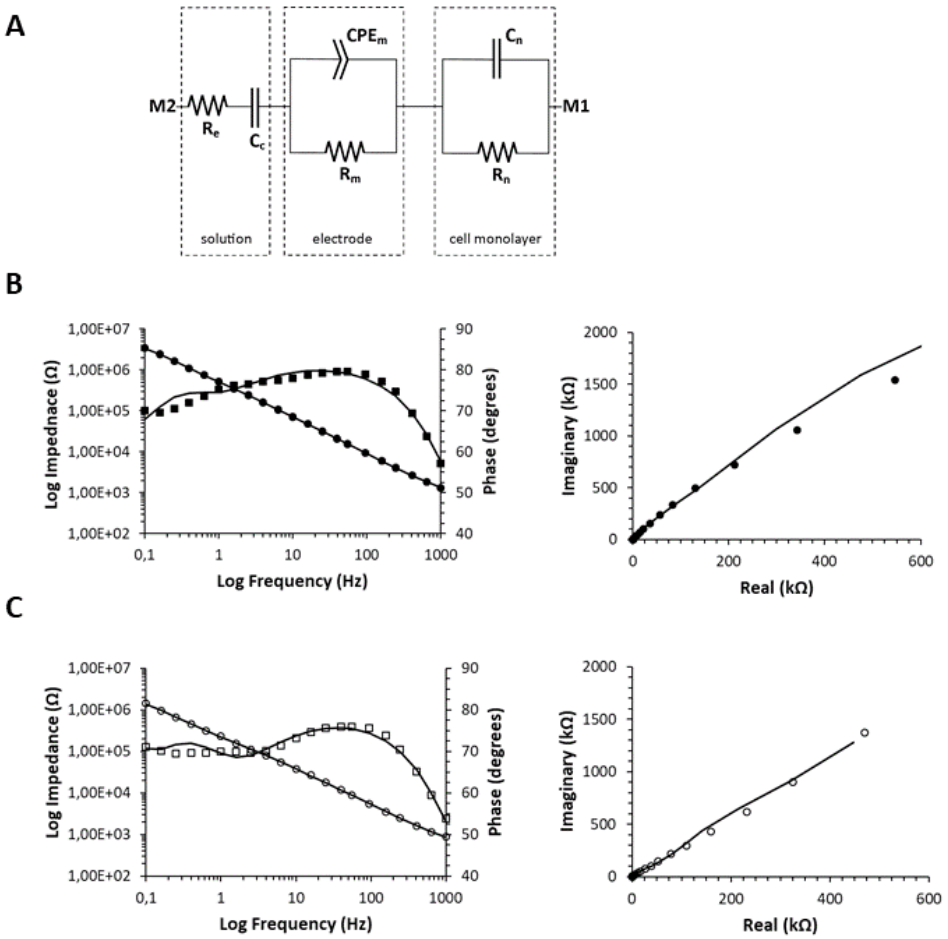

Figure 3. (A) The equivalent circuit used to model the EIS measurements. The paracellular resistance is represented by R_n and the capacitance of the cell monolayer is represented by C_n. The other components take into account the contributions of the electrodes (CPE_m, R_m) and the media solution (R_e, C_c). **(B)** Application the model to analyse the EIS measurement on RPTEC cells at day 1. The Bode Plot is shown on the left for the phase (■) and the impedance (●). The Nyquist plot is shown on the right. **(C)** Application the model to analyse the EIS measurement on 786-O cells at day 1. The Bode Plot is shown on the left for the phase (□) and the impedance (○). The Nyquist plot is shown on the right.

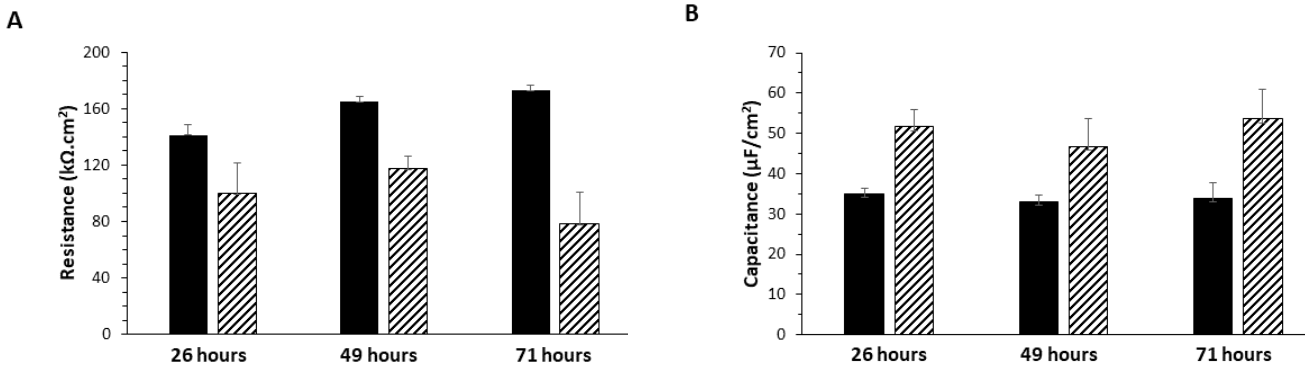

Figure 4. Resistance and capacitance of the cell monolayers obtained from modelling the EIS measurements. The times for measurements are the hours elapsed since the seeding of the cells, over 3 days. **(A)** Resistance of the cell monolayers taking into account the area of the measurement electrode (2.1 mm^2). The RPTEC cells are represented by the solid bars and the 786-O cells by the hatched bars. The error bars indicate standard error of the mean. **(B)** Capacitancee of the cell monolayers taking into account the area of the measurement electrode (2.1 mm^2). The RPTEC cells are represented by the solid bars and the 786-O cells by the hatched bars. The error bars indicate standard error of the mean.

using RStudio (v1.2.5033). This figure shows the capacitance and the resistance of the monolayers after several days in culture on the T10/microfluidic cartridges. At each time of the EIS measurement, (i) the resistance of the RPTEC cell monolayer was greater than that of the 786-O cells, and (ii) the capacitance of the RPTC cell monolayer was lower than that of the 786-O cells. It is important to note that the media solution in each well was changed after the EIS measurement on the 2nd day. Over the period of the 3 days, the resistance of the RPTEC and 786-O cell monolayers did not change significantly ($F = 1.167$, p = NS), although there seemed to be a tendency for a slight increase in the RPTEC. However, the resistance of the RPTEC cell monolayer was higher than that of the 786-O cell monolayer ($F = 5.566$, $p = 0.05$).There was no significant interaction effect between the time of measurement and the cell-type ($F = 1.698$, p = NS). Overall, the lower resistance of the 786-O cell monolayer suggested a decrease in the cell-cell cohesion of this cell-type. Since the tight junctions between individual cells control the cohesion of the cell monolayer, the lower resistance of the 786-O cell monolayer suggests that there may be a changed configuration of the tight junctions in the cancer 786-O cell monolayer compared to the normal RPTEC cell monolayer.

Over the period of the 3 days, the capacitance of both the RPTEC and 786-O cell monolayers did not change ($F = 0.053$, p = NS). However, the capacitance of the RPTEC cell monolayer was lower than that of the 786-O cell monolayer ($F = 12.912$; $p = 0.001$). There was no significant interaction effect between the time of measurement and the cell-type ($F = 0.237$, p = NS). At the frequency range of the EIS measurements this capacitance is a combination of the individual capacitances of the apical and basolateral membranes of the cells in the monolayers. The difference in capacitance between the RPTEC and 786-O cell monolayers suggests that the membrane properties were also different between the RPTEC and 786-O cells.

Discussion

We report here that the Tethapod, which is normally used for EIS measurements on tethered lipid bilayers (6), can be useful for assessing biological changes in cell cultures. The Tethapod is a swept frequency ratiometric impedance spectrometer for low-voltage (20 mV) AC impedance spectroscopy measurements over the frequency range from 0.125Hz to 1000Hz. Indeed, the Tethapod provides three advantages for the EIS measurements on the cell monolayers. Firstly, the large ground electrode faced the much smaller measurement electrode across a closed microfluidic channel of 100μm, which yielded homogeneous electric fields that were less sensitive to variations in the vertical cell position as compared to a configuration of coplanar electrodes on the same side of the channel (7). Secondly, the measurement electrodes have a small surface area (2.1 mm^2) and are included within an integrated microfluidic system that comprised 6 electrodes. This allowed 6 separate cell monolayers and/or control conditions to be measured simultaneously. Each electrode is accessed by separate microfluidic channels that facilitates the convenient seeding of the cells, the growth of the monolayer and the convenient removal of the media for sustained cell culture. Thirdly, in the frequency range of the Tethapod the paracellular resistance, between the cells, and the capacitance of the cell monolayer predominately contribute to the total impedance (8). In this frequency range the large cell capacitance is predominate in the current flow across the cell, and we can summate the apical and basolateral membranes as one capacitance (cell monolayer) that we use in modelling the EIS measurements.

The lower resistance that we measured for the cancerous (786-O) cell monolayer compared to the normal (RPTEC) cell monolayer suggested that the cancerous cell monolayer had an increased permeability compared to the normal cells. This would suggest that the barrier properties of the cancerous cell monolayer were reduced, which is probably not surprising given that the growth of cancerous cells is usually disordered (9). The higher capacitance that we measured for the cancerous (786-O) cell monolayer compared to the normal (RPTEC) cell monolayer suggested that the membranes of the cancerous cell monolayer were different to those of normal cells. This measured capacitance was a combination from the capacitances of the apical and basolateral membranes, but nonetheless the measured capacitance suggested a difference in either or both of these membranes in the cancerous cells. The frequency range for our EIS measurements precluded the influence of cytoplasm properties, since it has been reported that the cytoplasm conductivity becomes prevalent at frequencies approaching 10 MHz (10). The difference in capacitance that we measured could indicate, for example, differences in the composition of the phospholipids or the composition of membrane proteins that could have altered the dielectric properties of the cell membrane (11-13). The measurement of capacitance is sensitive to changes in the dielectric properties, and hence our measurements of capacitance may provide a measurement of the difference in composition of the membranes of cancerous cells compared to normal cells. Albeit for a different purpose, the specific membrane capacitance was shown to change during the differentiation of neural stem cells, which was due to changes in the expression of membrane proteins (14). It is likely that changes in the composition of the membranes of normal cells becoming cancerous may similarly induce changes in the dielectric properties of the cells. With this Tethapod system we were able to measure simultaneously both the differences in membrane properties of cell monolayers of cancer compared to normal cells, which may provide insights into the changes in composition of the membranes of these cells.

Our results of decreased resistance but increased capacitance for cancerous kidney epithelial cell monolayers has been previously observed in another cell-type. In that report, the authors found similarly to our measurements that the resistance of the normal skin cell monolayer (HaCaT) was higher than the cancerous cell monolayer (A431), but that the capacitance of the normal cell monolayer was quite similar to the cancerous cell monolayer (3). The measurements that we report here

might also provide information to further use these micro-EIS measurements for investigating the physiology of the adhesive properties of epithelial kidney cancer cells. Indeed, as the function of the kidneys depends on the maintenance of an epithelial barrier, the paracellular permeability to solutes and water might be modified in cancer. Thus, membrane properties of cancer cells identified by our measurements could lead to further investigations proteins known to have a major role into tight junctions between cells (15). As an example, claudin-2 a protein from tight junctions is highly expressed in kidney, liver, pancreas, stomach, and small intestine with a highest level in kidney. The presence of claudin-2 causes the formation of cation-selective channels that then increase the permeability between cells, whereas claudin-1 and claudin-4 decrease the permeability of the tight junctions (16). Thus, this device can be thereafter dedicated to study the specific role of one protein that could be incorporated in lipid bilayers.

Conclusion

We report that the Tethapod system, which was designed to determine the impedance properties of lipid bilayers, had a small measurement electrode surface area over which we could grow a monolayer that remained functionally viable for several days. To that purpose we have used normal epithelial cells from kidney (RPTEC) and a kidney cancer cell model (786-O). We demonstrate that the Tethapod system is compatible with the culture of cells 10,000 cells seeded for each of 5 measurement electrodes for simultaneous micro-EIS recordings. Furthermore, the range of frequencies for EIS measurements were tuned to examine easily the characteristics of the cell monolayer, including that we demonstrate significant differences in the paracellular resistance pathway between normal and cancer kidney epithelial cells. Thus, we conclude that this device has advantages for the study of cultured cells that include (i) the configuration of measurement and reference electrodes across a microfluidic channel, and (ii) the small surface area of measurement electrodes (2.1 mm^2) integrated in a microfluidic system. These characteristics might improve micro-impedance spectroscopy measurement techniques to provide a simple tool for further studies in the field of the patho-physiology of biological barriers.

Acknowledgement

This research was financially supported by a grant (CanDIES) from the French Ligue Contre le Cancer.

Conflict of interest statement

The authors declare no financial or commercial conflict of interest.

Ethical compliance

This article does not contain any studies involving human participants or animals performed by any of the authors.

References

1. Leva-Bueno J, Peyman SA, Millner PA. A review on impedimetric immunosensors for pathogen and biomarker detection. Med Microbiol Immunol 2020; 209:343-362.
2. Brosel-Oliu S, Abramova N, Uria N, Bratov A. Impedimetric transducers based on interdigitated electrode arrays for bacterial detection -a review. Anal Chim Acta. 2019; 1088:1-19.
3. Zhang F, Jin T, Hu Q, He P. Distinguishing skin cancer cells and normal cells using electrical spectroscopy. J Electroanal Chem, 2018; 823:531-536.
4. Valero A, Braschler T, Renaud P. A unified approach to dielectric single cell analysis: Impedance and dielectrophoretic force spectroscopy. Lab Chip, 2010; 10:2216-2225.
5. Cranfield C, Carne S, Martinac B, Cornell B. The assembly and use of tethered bilayer lipid membranes (tBLMs). Methods Mol Biol, 2015; 1232: 1232-1245.
6. Maccarini M, Gayet L, Alcaraz JP, Liguoria L, Stidder B, Cortès S, Watkins E, Lenormand JL, Martin DK. Function of recombinant OprF from Pseudomonas aeruginosa stably incorporated in supported lipid bilayers. Langmuir. 2017; 33:9988-9996.
7. Bürgel SC, Escobedo C, Haandbæk N, Hierlemann A. On-chip electroporation and impedance spectroscopy of single-cells. Sens Actuators B. 2015; 210:82-90.
8. Benson K, Cramer S, Galla H-J. Impedance-based cell monitoring: barrier properties and beyond. Fluids Barriers CNS, 2013; 10:5.
9. Czulkies BA, Mastroianni J, Lutz L, Lang S, Schwan C, Schmidt G, Lassmann S, Zeiser R, Aktories K, Papatheodorou O. Loss of LSR affects epithelial barrier integrity and tumor xenograft growth of CaCo-2 cells. Oncotarget. 2017; 8(23):37009-37022.
10. Gawad S, Cheung K, Seger U, Bertsch A, Renaud P. Dielectric spectroscopy in a micromachined flow cytometer: theoretical and practical considerations. Lab Chip, 2014; 4:241-251.
11. Vykoukal J, Vykoukal DM, Sharma S, Bescker FF, Gascoyne PRC. Dielectrically addressable microspheres engineered using self-assembled monolayers. Langmuir, 2003; 29:2425-2433.
12. Wiedman G, Herman K, SearsonP, Wimley WC,Hristova K. The electrical response of bilayers to the bee venom toxin melittin: evidence for transient bilayer permeabilization. Biochim Biophys Acta. 2013; 1828:1357-1364.
13. Andersson J, Fuller MA, Wood K, Holt SA, Köper I. A tethered bilayer lipid membrane that mimics microbial membranes. Phys Chem Chem Phys, 2018; 20:12958-12969.
14. Zhao Y, Liu Q, Sun H, Chen D, Li Z, Fan B, George J, Xue C, Cui Z, Wang J, Chen J. Electrical property characterization of neural stem cells in differentiation. PLos ONE. 2016; 11:e0158044.
15. Tang VW, Goodenough DA. Paracellular ion channel at the tight junction. Biophys J, 2003; 84:1660-1673.
16. Singh AB, Harris RC. Epidermal growth factor receptor activation differentially regulates claudin expression and enhances transepithelial resistance in Madin-Darby Canine Kidney Cells. J Biol Chem, 2004; 279:3543-3552.